

Supporting Information for Molecular-scale force measurement in a coiled-coil peptide dimer by electron spin resonance Stefano V. Gullà et al.

Synthesis and Purification of Coiled-Coil Peptide:

Materials Fmoc-Arg (Pbf)-Nova Syn TGA resin (0.23 mmole/g), 9-Fluorenylmethyl-oxycarbonyl-O-succinimide (Fmoc-OSu) and all the amino acids were purchased from Novabiochem, San Diego, CA. Triisopropylsilane (TIS), anisole, hexafluoro-2-propanol (HFIP), 30% ammonium hydroxide [NH₃ (aq.)], piperidine were purchased from Sigma-Aldrich, St. Louis, MO. 2,2,6,6-Tetramethylpiperidine-1-oxyl-4-carboxylic acid (TOAC) was purchased from Acros Organics, Belgium. Trifluoroacetic acid (TFA), 1-hydroxybenzo-triazole (HOBt), (2-(7-Aza-1H-benzotriazole-1-yl)-1,1,3,3-tetramethyluronium hexafluorophosphate (HATU), diisopropylethylamine (DIEA), N-Methyl-Pyrrolidone (NMP), dichloromethane (DCM) were purchased from Applied Biosystems, Foster City, CA. Acetic Anhydride (Ac₂O) and methyl-tert-butyl ether were purchased from Fisher Scientific, Pittsburgh, PA.

Procedure Solid phase peptide synthesis using Fmoc-protection chemistry was performed on a 433A Peptide Synthesizer from Applied Biosystems Inc., Foster City, CA. The 433A peptide synthesizer connected with UV-detector (wavelength 301nm) was used to monitor the Fmoc-removal from the N-terminus of the growing peptide. A locally modified version of the 0.1mmol Fast Fmoc Chemistry protocol in the SynthAssist 2.0 Software from Applied Biosystems (Foster City, CA) was used for optimal synthesis of the peptides. All amino acids were purchased in Fmoc protected as well as the side-chain protected forms for minimizing the unnecessary reactions during peptide synthesis.

Figure S1 shows the sequence of the leucine zipper region of the GCN4 yeast transcriptional activator that was synthesized. The N-terminal region includes 3 glycines not in the original sequence, which were added in order to extend the alpha helical structure at the N-terminus and avoid increased mobility of the terminal TOAC spin label.¹⁻⁴

The appropriate amounts of peptide resin (150-200mg) was treated with a suitable cleavage mixture (8.5mL TFA, 0.5mL TIS, 0.5mL anisole and 0.5mL distilled water) for 3 hrs to remove the side chains and detach peptide from the resin beads. The peptide was then filtered to remove the resins and precipitated in ice-cold methyl tert-butyl ether. The precipitated peptide was collected by centrifugation and vacuum dried overnight. Crude peptide was processed on an Amersham Pharmacia Biotech AKTA Explorer 10S HPLC controlled by unicorn (version 3) system software. The peptides were purified by Reversed Phase HPLC using protein C-4 semiprep (Vydac cat. # 214TP1010, 10µm, 10×250 mm) and protein C-4 prep (Vydac Cat # 214TP1022, 10µm, 22×250mm) columns. The HPLC solvent system consisted of of H₂O with 0.1% TFA for Solvent A and a mixture of 70% acetonitrile: 25% isopropyl alcohol : 5% H₂O: 0.1% TFA mixture for Solvent B. Since TFA converts nitroxide spin label into hydroxylamine form during peptide cleavage, the purified peptides were treated 3 hrs with 10 % aq. ammonia to regenerate the nitroxide spin label. The purity of the peptides was confirmed by matrix assisted laser desorption ionization time of flight (MALDI-TOF) mass spectrometry.

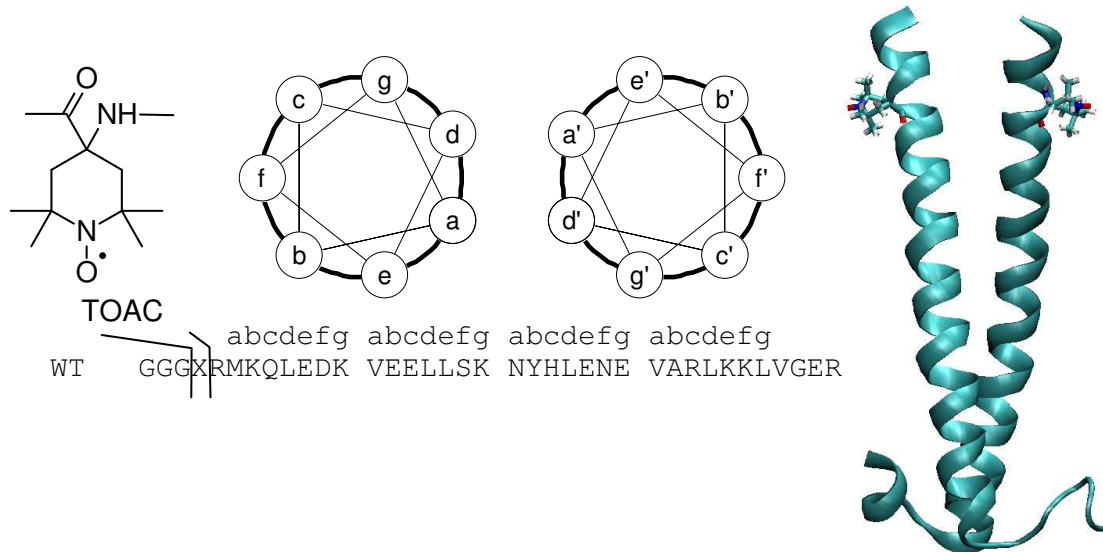


Figure S1. Coiled-coil leucine zipper structure investigated in this work, indicating structure and position of the TOAC spin label in the sequence and within the leucine zipper motif. Right: cartoon of the coiled-coil dimer conformation, showing the location TOAC labels (residue 248 in PDB ID)

ESR sample preparation

Lyophilized peptides were reconstituted in buffer of 40mM potassium phosphate, 50mM NaCl, 30% Sucrose at pH 7.0. Approximately 30 μ L of sample were placed in 3 mm OD glass capillaries for cw-ESR spectroscopy, and ~15 μ L were loaded into 1.8 mm ID capillaries for DEER spectroscopy.

cw-ESR Spectroscopy

cw-ESR spectra were obtained at room temperature in a Bruker EMX spectrometer fitted with a high sensitivity cylindrical cavity. The following acquisition parameters were used: $g = 2$ center field, modulation frequency 100 kHz, modulation amplitude 0.5 G, scan width 150 G.

Figure S2 shows a CW-ESR spectrum from the TOAC-labeled coiled-coil structure at pH 7. Dynamic parameters (*cf.* Figure 2 caption) were obtained by least-squares fitting of the slow-motional lineshape^{5,6} with consensus magnetic parameters for TOAC.^{3,7} The labeled coil-coil structure exhibited significantly anisotropic motion, with the principal diffusion axis (i.e. the long axis of the dimer) perpendicular to the magnetic x direction and approximately 30° away from magnetic z , consistent with the direction estimated from a molecular model (*cf.* Figure 2). Also shown in Figure 2 is the CD spectrum of the peptide, which demonstrates that the sample exists entirely as α helix, consistent with the Multiscore prediction of a coiled-coil conformation, where a score between 0.5 and 1.0 indicates probable coiled-coil formation.

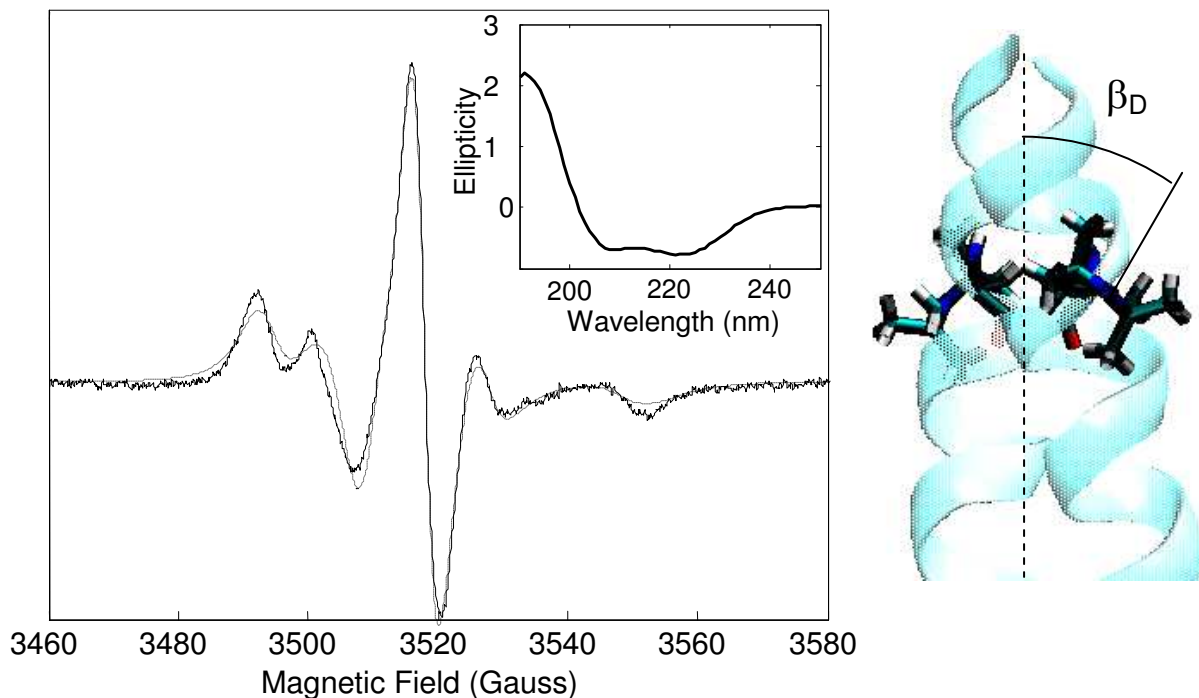


Figure S2: X-Band CW-ESR spectrum of the labeled coiled-coil dimer (model shown at right) at room temperature. Dotted line shows least-squares slow-motional lineshape. Least-squares values of the rotational diffusion constants parallel and perpendicular to the major axis of the molecule (shown by dashed line) were $R_{\parallel} = 1.8 \times 10^9 \text{ s}^{-1}$, $R_{\perp} = 1.9 \times 10^7 \text{ s}^{-1}$, with diffusion tilt angle $\beta_D = 25^\circ$. Fixed-value parameters in the fit were the electronic g -factor $(g_x, g_y, g_z) = (2.0085, 2.0056, 2.0020)$, ^{14}N hyperfine tensor $(A_x, A_y, A_z) = (21, 9.0, 105) \text{ MHz}$, inhomogeneous Gaussian linewidth 1.9 Gauss, and diffusion tilt angle $\alpha_D = 90^\circ$. *Inset:* CD spectrum of the peptide displaying the characteristic features of an alpha-helical coiled-coil.

DEER spectroscopy

DEER measurements were obtained on a locally constructed 17 GHz pulsed ESR instrument at the Center for Advanced ESR Technology (ACERT) at Cornell University. The measurements were carried out at a sample temperature of 65 K. Primary echoes at the detection frequency of 17.35 GHz were obtained using 16/32 ns pulses separated by 250 ns, applied at the low-field edge of the ESR spectrum. The primary echo amplitude was $\sim 3.0 \text{ V}$ (single-shot SNR ~ 150) measured at a signal gain of -15 dB corresponded to spin concentration of $\sim 300 \mu\text{M}$, referenced using $200 \mu\text{M}$ solution of 4-hydroxy-2,2,6,6-tetramethylpiperidine-N-oxyl in 50 wt% glycerol-water at the same conditions. The four-pulse DEER frequency setup was standard, utilizing a 32 ns pump π -pulse at a frequency separation of 70 MHz. With the instrument configuration used, the echo amplitude in DEER as a function of position of the pump pulse within the pulse sequence is known to be reproducible to within 0.3%, corresponding to less than 3% error in the extracted DEER signal. The DEER spectrum was collected as a function of pump pulse frequency at a selection of frequencies across the ESR spectrum, and was practically independent of the pump frequency.

The frequency domain DEER spectra reflect a frequency distribution given by

$$\nu = \frac{\mu_0 g_1 g_2 \beta^2 (3 \cos^2 \theta - 1)}{4\pi h r^3} \quad [1]$$

where g_1 and g_2 are the isotropic g -factors of each electron, β is the Bohr magneton, μ_0 is vacuum permeability, h is Planck's constant, r is the interspin distance, and θ is the angle between the magnetic field and the interspin vector.

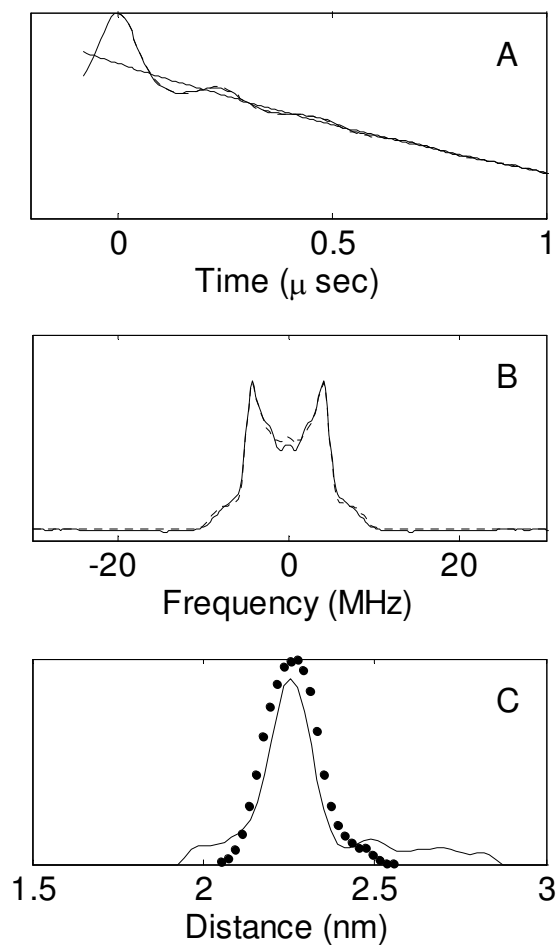


Figure S3. (A) Time domain DEER signal showing modulation from spin-spin interaction. (B) Frequency domain DEER signal showing characteristic Pake pattern of an isotropically distributed pair of dipoles, obtained by Fourier transform of the data in (A) after baseline subtraction (straight line); (C) Solid line shows distribution of distances between spin labels obtained by model-independent Tikhonov analysis of the DEER spectrum as described in the text. Symbols show distance distribution calculated from molecular dynamics using the adaptive biasing force method as described below

Adaptive Biasing Force (ABF) Molecular Dynamics Simulation

The adaptive biasing force (ABF) method was used as implemented in the NAMD molecular dynamics program.⁸ The starting coordinates of the coiled-coil dimer were obtained from the X-ray crystal structure coordinates of leucine zipper (LZ) portion (residues 243-281) of the yeast transcriptional activator GCN4⁹ (PDB entry 1YSA), with was solvated and equilibrated in a 50 Å×50 Å×70 Å cell using standard methods, and chloride ions added to neutralize the total charge. The simulations employed the CHARMM27 force-field,¹⁰ the particle mesh Ewald method¹¹ for electrostatic interactions, a switching function for van der Waals interactions with switching distance of 10 Å and a cutoff of 12 Å, and the ShakeH algorithm¹² to fix hydrogen bond lengths with a relative tolerance of 1.0×10^{-8} . Calculations were carried out using the Nosé-Hoover NPT ensemble¹³ at 1 atm and 298 K with a damping coefficient of 5 ps and a 2 fs integration time step. The reaction coordinate ξ was chosen as the distance separating the alpha carbon atoms of residue 248 (i.e., the TOAC label site) in the two chains, and was restricted to $10 \leq \xi \leq 35$ Å, allowing the peptide to evolve freely from closed to open state.

In the ABF calculation, the average force $\langle F_\xi \rangle$ along a selected (e.g. the spin-spin distance) is related to the derivative of the free energy $A(\xi)$:

$$\frac{dA(\xi)}{d\xi} = -\langle F_\xi \rangle \quad [2]$$

Over the course of an MD trajectory, the instantaneous force along ξ is tabulated as a function of ξ in small bins of width $\delta\xi$, from which the derivative $dA(\xi)/d\xi$ (and thus the free energy $A(\xi)$) may be estimated. Optionally, one may apply an adaptive biasing force (ABF) that cancels the instantaneous force in order to overcome local free energy barriers and ensure uniform sampling of the ξ coordinate. $A(\xi)$ is then related to the probability $P(\xi)$ of finding the system at coordinate ξ by the PMF equation:^{14,15}

$$A(\xi) = -k_B T \ln P(\xi) + A_0 \quad [3]$$

in which A_0 is the standard-state free energy. If one takes $P(\xi)$ to be the spin label distance distribution measured by DEER, one may work backwards from the experimental $P(\xi)$ to find $A(\xi)$ from Equation 3, and then numerically calculate the derivative $dA(\xi)/d\xi$ to find the average force on the coiled-coil peptide.

As stated above, the curve calculated from MD-ABF reflects the distance between the alpha carbons of residue 248, the labeling site. Since the DEER experiment measures distances between the electron spins, the calculated curve was shifted by 0.77 nm, which corresponds to exactly twice the distance between the backbone C_α and the midpoint of the N—O bond of each spin label as measured from the molecular model.

References for Supporting Material

- (1) Hanson, M. P.; Martinez, G. V.; Millhauser, G. L.; Formaggio, F.; Crisma, M.; Toniolo, C.; Vita, C. *Pept.: Chem., Struct. Biol., Proc. Am. Pept. Symp., 14th* **1996**, 533-534.
- (2) Hanson, P.; Anderson, D. J.; Martinez, G.; Millhauser, G.; Formaggio, F.; Crisma, M.; Toniolo, C.; Vita, C. *Mol. Phys.* **1998**, *95*, 957-966.
- (3) Inbaraj, J. J.; Cardon, T. B.; Laryukhin, M.; Grosser, S. M.; Lorigan, G. A. *J Am Chem Soc.* **2006** *128*, 9549-9554.
- (4) Inbaraj, J. J.; Laryukhin, M.; Lorigan, G. A. *Journal of the American Chemical Society* **2007**, *129*, 7710-7711.
- (5) Budil, D. E.; Earle, K. A. In *Advanced ESR Methods in Polymer Chemistry*; Schlick, S., Ed.; John Wiley & Sons: New York, 2006, p 53-83.
- (6) Budil, D. E.; Lee, S.; Saxena, S.; Freed, J. H. *J. Magn. Reson., Ser. A* **1996**, *120*, 155-189.
- (7) Nesselov, Y. E.; Karim, C. B.; Song, L.; Fajer, P. G.; Thomas, D. D. *Biophysical Journal* **2007**, *93*, 2805-2812.
- (8) Phillips, J. C.; Braun, R.; Wang, W.; Gumbart, J.; Tajkhorshid, E.; Villa, E.; Chipot, C.; Skeel, R. D.; Kale, L.; Schulten, K. *Journal of Computational Chemistry* **2005**, *26*, 1781-1802.
- (9) Ellenberger, T. E.; Brandl, C. J.; Struhl, K.; Harrison, S. C. *Cell* **1992**, *71*, 1223-1237.
- (10) MacKerell, A. D.; Bashford, D.; Bellott, M.; Dunbrack, R. L.; Evanseck, J. D.; Field, M. J.; Fischer, S.; Gao, J.; Guo, H.; Ha, S.; Joseph-McCarthy, D.; Kuchnir, L.; Kuczera, K.; Lau, F. T. K.; Mattos, C.; Michnick, S.; Ngo, T.; Nguyen, D. T.; Prodhom, B.; Reiher, W. E.; Roux, B.; Schlenkrich, M.; Smith, J. C.; Stote, R.; Straub, J.; Watanabe, M.; Wiorkiewicz-Kuczera, J.; Yin, D.; Karplus, M. *J. Phys. Chem.* **1998**, *102*, 3586-3616.
- (11) Darden, T.; York, D.; Pedersen, L. *J. Chem. Phys.* **1993**, *98*, 10089-10092.
- (12) van Gunsteren, W. F.; Berendsen, H. J. C. *Molecular Physics* **1977**, *34*, 1311-1327.
- (13) Martyna, G. J.; Tobias, D. J.; Klein, M. L. *J. Chem. Phys.* **1994**, *101*, 4177-4189.
- (14) Darve, E.; Pohorille, A. *Journal of Chemical Physics* **2001**, *115*, 9169-9183.
- (15) Otter, W. K. D.; Briels, W. J. *Molecular Physics* **2000**, *98*, 773-781.